JB
Journals.ASM.org

The Genome of *Pseudomonas fluorescens* Strain R124 Demonstrates Phenotypic Adaptation to the Mineral Environment

Michael D. Barton,[a] Michael Petronio,[b] Juan G. Giarrizzo,[c]* Bethany V. Bowling,[d] Hazel A. Barton[a]

The University of Akron, Department of Biology, Akron, Ohio, USA[a]; The University of Cincinnati, Department of Biological Sciences, Cincinnati, Ohio, USA[b]; Environmental and Molecular Toxicology, Oregon State University, Corvallis, Oregon, USA[c]; Northern Kentucky University, Biological Sciences, Highland Heights, Kentucky, USA[d]

Microbial adaptation to environmental conditions is a complex process, including acquisition of positive traits through horizontal gene transfer or the modification of existing genes through duplication and/or mutation. In this study, we examined the adaptation of a *Pseudomonas fluorescens* isolate (R124) from the nutrient-limited mineral environment of a silica cave in comparison with *P. fluorescens* isolates from surface soil and the rhizosphere. Examination of metal homeostasis gene pathways demonstrated a high degree of conservation, suggesting that such systems remain functionally similar across chemical environments. The examination of genomic islands unique to our strain revealed the presence of genes involved in carbohydrate metabolism, aromatic carbon metabolism, and carbon turnover, confirmed through phenotypic assays, suggesting the acquisition of potentially novel mechanisms for energy metabolism in this strain. We also identified a twitching motility phenotype active at low-nutrient concentrations that may allow alternative exploratory mechanisms for this organism in a geochemical environment. Two sets of candidate twitching motility genes are present within the genome, one on the chromosome and one on a plasmid; however, a plasmid knockout identified the functional gene as being present on the chromosome. This work highlights the plasticity of the *Pseudomonas* genome, allowing the acquisition of novel nutrient-scavenging pathways across diverse geochemical environments while maintaining a core of functional stress response genes.

Genomics has revolutionized the way we study microorganisms in the environment; in the postgenomic era, it is possible to describe the enzymatic pathway corresponding to metabolic pathways that are only hypothesized (1) or to predict the environmental function of uncultivated bacterial phyla based on single-cell isolation and genomic amplification (2, 3). The result has been a profound change in our understanding of microbial interactions and processes; however, not all environments have benefited from this revolution. At the intersection of microbiology and geology, comparative genomics has yet to examine how the interaction between microbes and minerals leads to genomic adaptation (4). As a result, numerous fundamental questions remain to be answered, such as what is the role of microorganisms in mineral precipitation and weathering (5, 6).

In this study we examined the genome of an organism isolated from a predominantly mineral environment, using a cave-isolated *Pseudomonas* strain as a model. Due to their ubiquitous distribution in terrestrial environments and association with opportunistic infections, pseudomonads have been studied for many years, and a large number of representative genomes exist: 37 completed projects within the genus *Pseudomonas*. Among the hundreds of bacterial species we have isolated from cave environments, we decided to examine the genomic adaptations of *Pseudomonas fluorescens* to this mineral environment. *P. fluorescens* is an advantageous organism for such studies, as we have isolated representatives from numerous cave environments, across a broad geographical range and under diverse geochemical conditions, arguing for the ubiquitous nature of this species in caves. There are also five reference genomes in the *P. fluorescens* subgroup that allow comparative analyses. In this study, we compared the genome of *P. fluorescens* R124 against the genomes of *P. fluorescens* Pf0-1 and SBW25, *P. protegens* Pf-5, and *P. aeruginosa* PAO1 (7, 8, 9, 10). These previously sequenced isolates were collected from a loamy agricultural soil (11), a cotton plant rhizosphere (12), the leaf of a sugar beet plant (13), and an infected wound (14), respectively.

Our assembled and annotated sequence data suggest that despite remarkable differences in local environment, the *P. fluorescens* R124 genome demonstrates close similarity with the genomes of its plant and soil relatives, although horizontal gene transfer has led to the accumulation of metabolic genes and a novel plasmid. By comparing its phenotypic characteristics with those of *P. fluorescens* Pf0-1 and SBW25, we also found that R124 has acquired numerous metabolic pathways for nutrient scavenging, as well as expressing a twitching-motility phenotype that may aid it in the exploration of a two-dimensional mineral space. This study describes only the second genome of a cave microorganism (15), and the first where genomic adaptations have a demonstrated phenotype.

MATERIALS AND METHODS

Strain isolation and growth conditions. *P. fluorescens* R124 was isolated from a tepui orthoquartzite sandstone cave in the Guiana Shield in South America. The isolation medium was nutrient agar containing 25 mg/liter of chemically extracted humic acids from potting soil (16). The organism was collected from the ceiling of the cave ~500 m from the entrance and

Received 12 July 2013 Accepted 22 August 2013
Published ahead of print 30 August 2013
Address correspondence to Hazel A. Barton, bartonh@uakron.edu.
* Present address: Juan G. Giarrizzo, Department of Microbiology, Oregon State University, Corvallis, Oregon, USA.
M.D.B. and M.P. contributed equally to this work.
Supplemental material for this article may be found at http://dx.doi.org/10.1128/JB.00825-13.

doi:10.1128/JB.00825-13

~25 m below the surface. The temperature of the sample site was 11.4°C, with a relative humidity of 99.6%. The chemistry of the rock was determined to be 96% Si (in the form of SiO_2), 3% Al, 0.12% Fe(III), and 0.04% P via X-ray fluorescence using a Bruker S4 Pioneer X-ray spectrophotometer. Various other metals (Cu, Mn, Ni, Co, etc.) were detected in trace amounts (1 to 20 ppm). Ammonia and nitrite were also detected.

The orthoquartzite nature of the cave limits surface-derived organic carbon and energy sources percolating into the cave system; however, an intermittent stream from the surface allows the periodic introduction of plant detritus in the form of soluble organic matter (SOM; 40 mg/liter). The *P. fluorescens* strain was single-colony isolated and maintained in tryptic soy broth/glycerol stock mixtures (4:1) at −80°C. To ensure that no contaminating species were introduced during DNA isolation, the strain was grown on a 50% tryptic soy agar plate for 48 h at 37°C before being scraped from the plate for DNA isolation. The organism identity was confirmed by sequencing the small ribosomal subunit 16S gene using the 8f and 1391R primers (17).

To measure metal homeostasis, we grew each strain in a minimal medium supplemented with the test metal. As M9 minimal medium contains phosphate which forms a metal-phosphate precipitate in the presence of divalent metal cations, we used a 4-(2-hydroxyethyl)-piperazine-1-ethanesulfonic acid (HEPES)-buffered medium that supported the growth of all strains tested. This medium contained 50 M HEPES (pH 7.0), 5% (wt/wt) tryptic soy broth, 0.5% NaCl, 1 mM $MgCl_2$, and 0.3% glucose. The metals tested (Fe, Cu, Ni, and Zn) were supplemented from 100 mM stocks of $FeSO_4$, $FeCl_3$, $CuCl_2$, $CdCl_2$, $NiCl_2$, and $ZnSO_4$. Cultures were inoculated to an optical density at 600 nm (OD_{600}) of 0.020 from an overnight culture grown in the base minimal medium. All cultures were grown at room temperature (20°C) with shaking at 200 rpm for 12 h. Optical density (OD_{600}) was monitored using a Hach DR 2800 spectrophotometer (Hach Company, Loveland, CO).

Sequencing, annotation and assembly. The *P. fluorescens* R124 genome was sequenced using a Roche GS Titanium at the University of Kentucky Advanced Genetic Technologies Centre (www.uky.edu/Centers/AGTC/). The DNA was sequenced as a mixture of shotgun and 2-kb paired-read fragments to provide both uniform genome coverage and paired-read assembly (18). Sequencing reads were assembled using the Roche De Novo genome assembler (Newbler). The assembled contigs and scaffolds were annotated using the Integrated Microbial Genomes (IMG) resource (19).

The assembled contigs and scaffolds were aligned to the *P. fluorescens* Pf0-1 genome (9) using Nucmer (20). The strain *P. fluorescens* Pf0-1 was used as a reference, since it was the most phylogenetically similar strain at the time of assembly (see Fig. 1). Pairwise comparison of *P. fluorescens* R124 scaffolds with other available genomes also confirmed *P. fluorescens* Pf0-1 as the most similar in genome sequence (see Fig. 3).

The *P. fluorescens* R124 draft genome sequence was generated from the reference alignment using the Genomer software (21, 22), and the origin of replication was estimated from sequence identity to *P. fluorescens* Pf0-1.

Estimation of *Pseudomonas* phylogeny. Mulet et al. (23) used the partial sequences of three protein-coding genes, *gyrB*, *rpoB*, and *rpoD*, along with the 16S rRNA gene to generate a phylogenetic tree. To determine the phylogenetic location of *P. fluorescens* R124 we used these three full-length protein sequences from available *Pseudomonas* genomes to build a protein sequence alignment. Each protein sequence was aligned separately with MAFFT (24, 25), and then the sequences were concatenated to build a larger alignment, which was filtered using Gblocks (26). The phylogenetic tree was estimated using PhyloBayes (27) and a general time-reversible model (28) with 8 Markov chain Monte Carlo (MCMC) chains until a steady-state distribution was reached. The initial burn-in was discarded from each MCMC chain, and a consensus tree was built from the remaining trace.

Plasmid curing. The pMP-R124 plasmid was cured as described by Chin et al. (29). Briefly, *P. fluorescens* R124 was grown in subinhibitory levels of ethidium bromide (100 μg/ml) for 24 h at 37°C. Surviving cells were then plated on brain heart infusion (BHI) medium, whereupon colonies were picked and screened for the loss of the plasmid via PCR using two sets of primers unique to the plasmid. These primer sets were 5′-CACTGGTGGAACGCCAGAGCC-3′ (forward) and 5′-CGATCCTTAACCGACACCCGG-3′ (reverse) (located at 41657 to 41899) and 5′-CGGCGCGATCGGCCCTCT-3′ (forward) and 5′-CGAGGCCGCCGGCTTCGC-3′ (reverse) (located at 41838 to 41155).

Identification of horizontally gene transfer regions. Potential horizontal gene transfer (HGT) regions in the *P. fluorescens* genome were identified using the OligoWords tool to detect differences in local versus global tetranucleotide variance (30, 31). A generalized extreme value distribution was used to select the HGT regions with a variance in tetranucleotide usage with a probability of 0.05 or less. The extreme value distribution was modeled using the R statistical programming language (32). These candidate regions were filtered to select for those containing less than three genes or which sequence similarity indicated were not present in any other sequenced *Pseudomonas* genomes. This identified HGT regions unique to *P. fluorescens* in the *Pseudomonas* genus and thereby genes likely unique to the environment.

Processing of Biolog growth data. Metabolic phenotype assays were carried out using the phenotype microarray (PM) system (Biolog, Hayward, CA) as previously described for plates PM1 to PM4 (33). Growth was carried out in M9 minimal medium with 25 mM sodium pyruvate as a carbon source and the addition of 0.005% (vol/vol) tryptic soy agar (TSA) broth to the medium (this low concentration of TSA does not affect the C/N/P/S assays of the Biolog System [B. Bochner, personal communication]). For the various C/N/P/S PM plates, each of the carbon, nitrogen, phosphorus, and sulfur sources was omitted from the M9 medium as appropriate. The plates were incubated for 4 days at room temperature. Metabolic activity was measured by absorbance at 590 nm minus the background absorbance at 750 nm. The empty control well value (well A1) was then subtracted from the value for the other wells in the same plate.

Twitching motility assays. Twitching motility assays of *P. fluorescens* strains R124, Pf0-1, and SBW25, and *P. aeruginosa* PAO1 were performed using methods previously described (34, 35), testing several different media to induce twitching, including 1% and 50% LB (nutrient limitation and salt), 1% BHI (nutrient limitation), and 1% King's B (iron limitation) media (36). The agar concentrations for each medium were, respectively, 1.5%, 1.5%, and 2%. Media were obtained from Becton, Dickinson Company. Single colonies were stab inoculated to the bottoms of agar plates using a sterile toothpick and grown for up to 120 h. Zones of twitching motility were observed by removing agar and staining the plates with 1% crystal violet for 10 to 15 min.

Nucleotide sequence accession number. The annotated genome sequence of *P. fluorescens* R124 was deposited in GenBank under accession number CM001561.

RESULTS

Sequencing and assembly. Assembly of the *P. fluorescens* R124 Roche/454 sequencing reads resulted in eight major scaffolds and a number of unscaffolded contigs with an average assembled depth of 24 reads. Seven of the eight scaffold sequences aligned to the *P. fluorescens* Pf0-1 reference genome. Two assembled sequences aligned to the reference genome in five distinct locations, indicating that they represent likely repeat regions that have been artificially collapsed into single contigs by the assembly process. Sequence similarity searches using BLAST suggested these repeat regions contained rRNA genes. PCR and additional *in silico* alignment of sequencing reads generated 42 additional sequences to join contigs or extend the length on assembled contigs. The final length of the draft genome was ~6.3 Mbp with 99.5% estimated ungapped coverage. The genome assembly is summarized in Table S1, and minimum information about a genome sequence

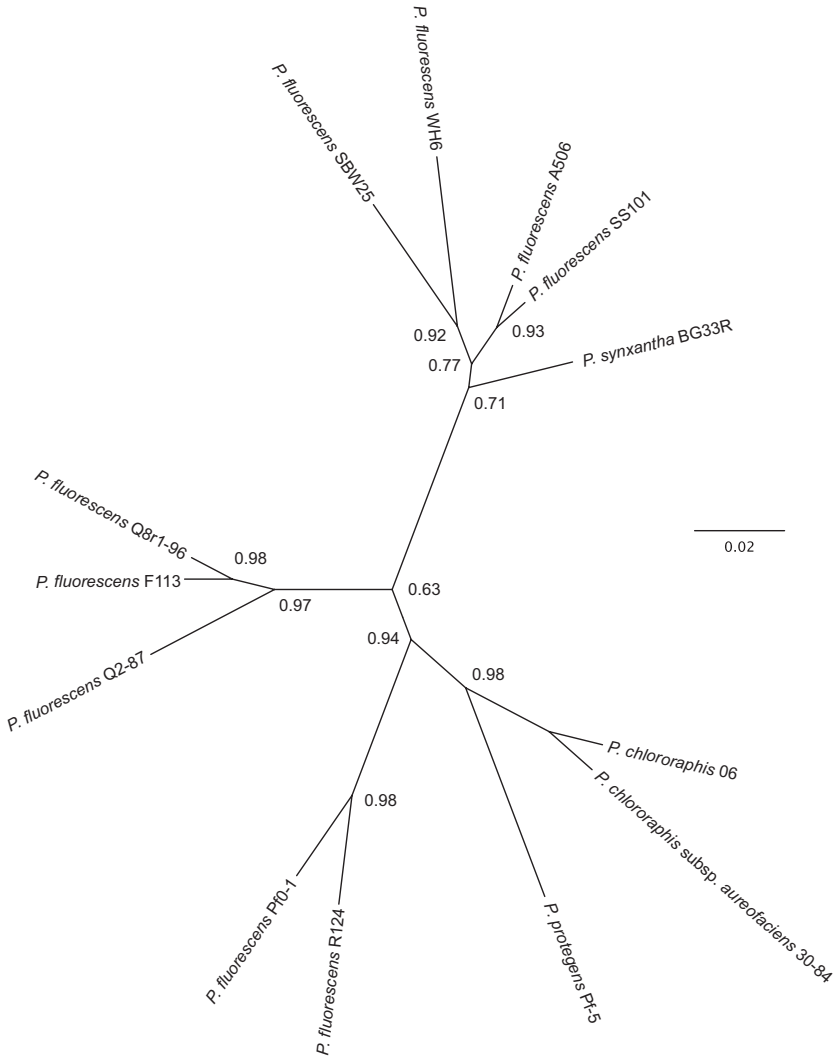

FIG 1 Unrooted phylogeny for the sequenced *P. fluorescens* strains and related species. The phylogeny was estimated from the concatenated alignment of three protein sequences: GyrB, RpoB, and RpoD. Bootstrapped support values are shown on each node.

(MIGS) is provided in Table S2 in the supplemental material (37). One 43-kbp scaffold sequence did not align with *P. fluorescens* Pf0-1 but instead aligned with two *Pseudomonas syringae* plasmids: 1448A-small (38) and ES4326 pPMA4326A (39). PCR primers generated to amplify outward from each end of the contig generated a PCR product with sequences overlapping the 5′ and 3′ ends of the contig, indicating that this sequence is closed and represents a complete plasmid.

Comparison with other *Pseudomonas* genomes. A phylogenetic tree was estimated for *P. fluorescens* R124 using a multilocus alignment of three protein sequences. The tree for the immediate *P. fluorescens* phylogeny is shown in Fig. 1. The full estimated phylogeny for all included *Pseudomonas* strains is shown in Fig. S3 in the supplemental material. These estimated phylogenies indicate that *P. fluorescens* R124 is grouped with the other *P. fluorescens* strains with moderate bootstrap support (62% at the branch point). We therefore classify R124 as a *P. fluorescens* strain, although further expansion of the pseudomonad phylogeny may demonstrate that both strains R124 and Pf0-1 may branch as a new species within the genus.

Our initial hypothesis is that the nutrient limitation of a cave environment would lead to genome streamlining (minimizing the nutrient and energy investment in genome replication). We therefore compared the length and gene density of genes in the *P. fluorescens* R124 genome with those in other sequenced *P. fluorescens* strains and representative pseudomonads. The results (Fig. 2) demonstrate that *P. fluorescens* R124 is not the smallest representative genome for *P. fluorescens*, with numerous other smaller *Pseudomonas* genomes observed. The median number of genes per kilobase was calculated for these *Pseudomonas* genomes, excluding R124. The median gene density, 0.906 gene/kb (Fig. 2, dashed line), was greater than that of R124 (0.841 gene/kb), suggesting a reduced gene density in R124.

To examine genome conservation between the *P. fluorescens* Pf0-1 and SBW25, *P. protegens* Pf-5, and *P. fluorescens* R124 genomes, the four genome sequences were aligned. *P. protegens* Pf-5 was included in this comparative analysis, as at the time of assembly it was still classified within the *P. fluorescens* group (8). The results of this analysis are shown in Fig. 3 and demonstrate the regions of similarity between *P. fluorescens* R124 and

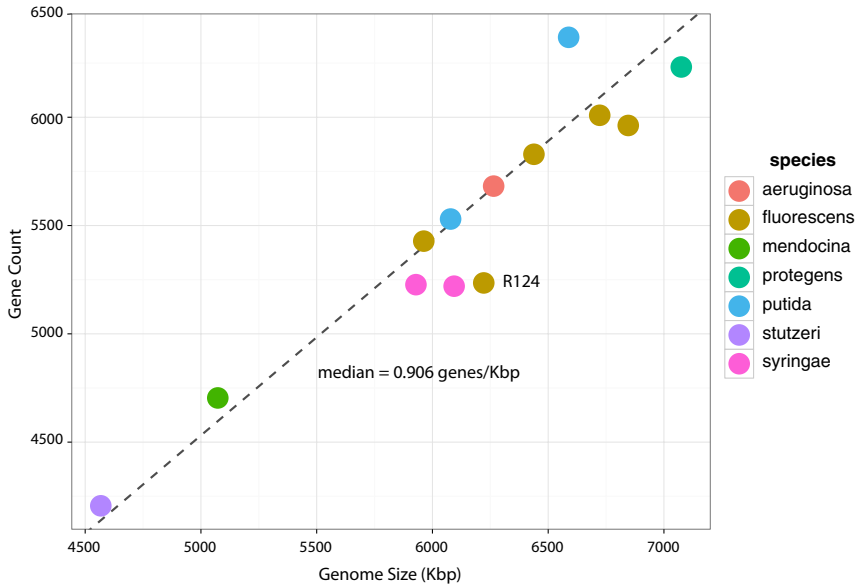

FIG 2 Comparison of *Pseudomonas* genome sizes and gene counts. Each point represents a *Pseudomonas* genome, with species indicated by color. *P. fluorescens* R124 is labeled. The dashed line indicates the median gene density for the genomes (excluding *P. fluorescens* R124), with the intercept through the origin. The accession numbers for the organisms compared are AE004091, CP000094, CP000076, AM181176, AM235768, CP000680, CP000926, CP000744, CP000304, CP000058, and CP000075.

the three reference genomes. Figure 3A demonstrates a linear relationship between *P. fluorescens* R124 and the reference genomes in the regions of 0 to 2 Mbp and 4 to 6 Mbp, indicating a large amount of sequence conservation and suggesting that the genomic regions around the origin of replication in *P. fluorescens* R124 share synteny with the other *P. fluorescens* genomes. Despite this similarity, our results indicate a large region of genomic rearrangement and low sequence similarity

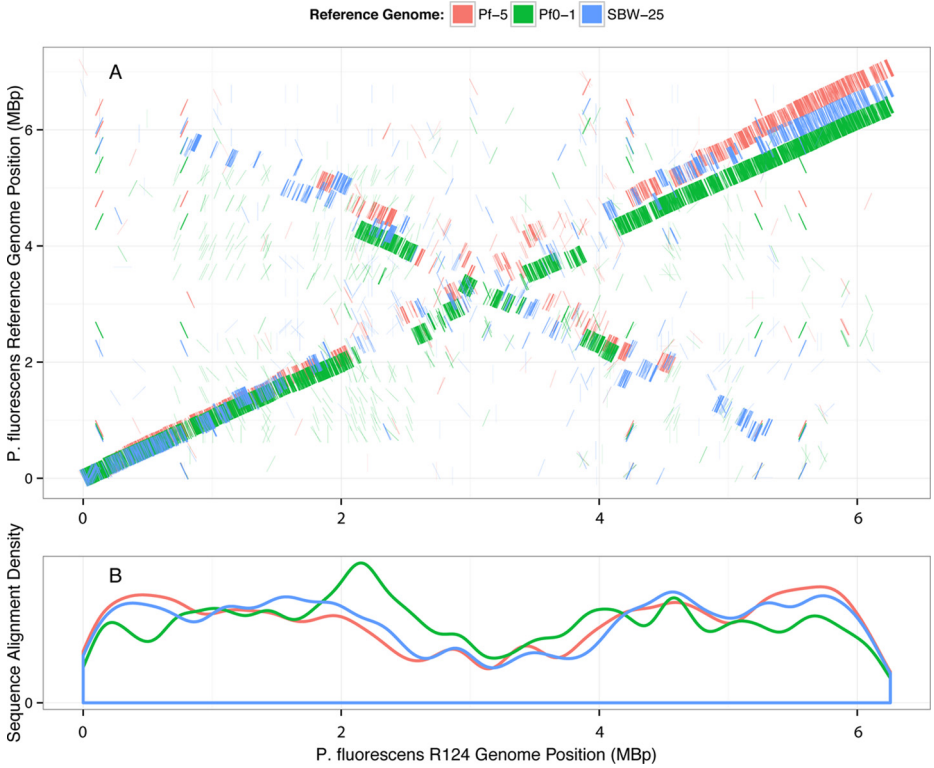

FIG 3 Pairwise comparison of the *P. fluorescens* R124 genome with three other *Pseudomonas* genomes; reference genomes are indicated by separate colors. The upper plot (A) shows the *P. fluorescens* R124 genome on the *x* axis, with the reference genome on the *y* axis. Each point on the upper plot represents a region of sequence similarity between the two genomes. The lower plot (B) shows the density of sequence similarity to *P. fluorescens* R124 compared to the reference genome.

around the 2- to 4-Mbp region (Fig. 3). This is highlighted by the lack of a linear relationship between the two axes in Fig. 3A and a low degree of conservation density (Fig. 3B). This suggests that the *P. fluorescens* genome may be more plastic in the regions furthest from the origin of replication.

The number of protein-encoding gene families shared between *P. fluorescens* R124 and the other three genomes was estimated using sequence alignment. The numbers of shared genes between *P. fluorescens* R124 and each of the other genomes are as follows: *P. fluorescens* Pf0-1, 2,893 (50.6%); *P. protegens* Pf-5, 2,709 (44.4%); *P. fluorescens* SBW25, 2,615 (44.2%). The total estimated number of gene families shared between all four compared genomes is 2,385. These results correspond to previous analysis showing that *P. fluorescens* and related species have diverse genomes (9).

Horizontal gene transfer. In order to identify potential regions of horizontal gene transfer (HGT) in the *P. fluorescens* R124 genome, we examined variance in tetranucleotide (4-mer) usage (30, 31). This approach detected 26 possible HGT regions, nine of which contained genes demonstrating no sequence similarity to other genes within the pseudomonads. (The analysis of these regions is summarized in Table S4 in the supplemental material.) Many of the predicted horizontal gene transfer regions contained genes with either no match or very low sequence similarity to genes identified using protein BLAST searches, and the functions of these genes therefore remain unknown. Nonetheless, three candidate HGT regions (regions 3, 6, and 7; see Table S4) contained genes that demonstrated sequence similarity to genes involved in carbohydrate and energy metabolism. These included genes for four glycosyltransferases, a triose-phosphate isomerase, a phosphoketolase, a fructose-bisphosphate aldolase, and an acetyl coenzyme A (acetyl-CoA) synthetase. Given that these genes are located in HGT regions originating outside the *Pseudomonas* genus, this highlights the possible selection pressures for additional catabolic pathways involved in energy metabolism in this environment.

We attempted to determine whether these regions of horizontal gene transfer gave *P. fluorescens* R124 the increased metabolic flexibility necessary to grow within a nutrient-limited cave environment. To do this, we compared the growth of R124 with its soil-isolated relatives using the comparative Biolog phenotypic microarray assay system (40). While we were able to successfully grow *P. fluorescens* SBW25 and Pf0-1, and *P. aeruginosa* PAO1 in the provided If-0a GN/GP base inoculating fluid, *P. fluorescens* R124 would not grow in this basal medium. We therefore used M9 minimal medium for growth, which is compatible with the Biolog system. Growth was analyzed in plates PM1 to PM4, which compare growth of *P. fluorescens* R124, SBW25, and Pf0-1 against that of *P. aeruginosa* PAO1, used as a control, in various carbon, nitrogen, phosphorus, and sulfur sources. The results demonstrated the growth of R124 in a number of carbon, nitrogen, phosphorus, and sulfur sources that could not be readily utilized by the other strains and species (Table 1). Of the 50 nutrient sources uniquely used by R124, many appear to be produced from the breakdown of biogenic polymers, sugars, carboxylic acids, and precursor molecules associated with microbial metabolism, including glucosamine, octopamine, mannitol, acetoacetic acid, galacturonic acid, malonic acid, hydroxylamine, allantoin, lanthionine, and lipoamide (Table 1). *P. fluorescens* R124 has also acquired the ability to grow on more obscure carbon sources, such as tyramine (an aromatic amine derived from tyrosine), β-D-allose (a rare epimer of glucose), arbutin (a glycosylated hydroquinone), and D-psicose (a rare carbohydrate derived from an antibiotic). Of particular note is the observation that several nucleosides/nucleotides (guanine, thymine, thymidine, and uracil) and nucleotide precursors (ribose, carbamyl phosphate, cystathionine, and allantoin) can serve as carbon and nitrogen sources, which could suggest pathways for the catabolism of nucleotides and polynucleotides (Table 1).

Metal homeostasis and nitrogen metabolism. Given the geochemically complex environment found within caves, we considered the possibility that these conditions led to increased adaptation in metal homeostasis in *P. fluorescens* R124. We therefore attempted to identify any homologs or missing or novel genes within metal-scavenging pathways of the *P. fluorescens* R124 genome in relation to comparable *P. fluorescens* strains. Moon et al. (41) identified 29 genes involved in siderophore production within *P. fluorescens* SBW25, Ravel and Cornelis (42) identified 30 genes in *P. fluorescens* Pf0-1, and Hartney et al. described 45 genes in *P. protegens* (43); we used these genes to comparatively search *P. fluorescens* R124 for the corresponding pathways. Comparison of the co-occurrence and sequence similarity of siderophore genes across the four genomes identified seven likely gene sets (see Table S5 and Fig. S6 in the supplemental material). The only group of siderophore genes in *P. fluorescens* R124 exhibiting divergence was a cluster of genes (I1A_001810, I1A_001811, I1A_001812, I1A_001813, I1A_001814, and I1A_001815) associated with nonribosomal peptide synthases (NRPS) (see Fig. S6 and Table S7 in the supplemental material). These genes showed a lower sequence identity (~40% to 50%) to the corresponding ortholog in the other *P. fluorescens* genomes than to other iron homeostasis genes (~73%) and appear to encode a lipopeptide, rather than a siderophore, structure.

The copper, nickel, zinc, cobalt, and cadmium metal homeostasis systems previously observed in *Pseudomonas* species (44–47) were also compared. (Table S7 in the supplemental material summarizes the sequence analysis of the *P. fluorescens* orthologs in these pathways.) The results of these analyses demonstrate that the genes in these metal uptake systems are conserved across the four *P. fluorescens* genomes, regardless of the environment from which the organism was isolated. In order to test whether this was represented in the phenotype, we examined the metal tolerance of *P. fluorescens* R124, Pf0-1, and SBW25 and *P. aeruginosa* PAO1 grown in liquid culture (Fig. 4). The data demonstrate similar levels of resistance to metal toxicity by *P. fluorescens* R124 to the other pseudomonads. If any difference can be discerned, it is that the environmental isolates (*P. fluorescens* R124, Pf0-1, and SBW25) demonstrate slightly higher levels of metal resistance than the clinical strain (*P. aeruginosa* PAO1).

Another potential stressor in cave environments is nitrogen limitation, which can influence community structure in subsurface environments (48), although both NH_4^+ and NO_3^- were detected in trace levels at the site of *P. fluorescens* R124 collection. Pseudomonads contain a number of different pathways for nitrogen utilization and are known for their denitrification capabilities, although the genes for nitrogen fixation (*Pseudomonas stutzeri nif* [49]) and nitrification (*Pseudomonas putida* [50]) are less common. Using BLAST, we examined the *P. fluorescens* R124 genome for genes involved in nitrogen metabolism; however, no gain of function was observed beyond the capabilities observed for *P. fluorescens* SBW25 and Pf0-1 (data not shown).

TABLE 1 Comparison of growth of *P. fluorescens* R124 with that of other pseudomonads using the Biolog phenotypic array

Chemical	Nutrient type	Growth of *Pseudomonas* strain[a]			
		PAO1	Pf0-1	SBW25	R124
L-Arabinose	C source	−0.563	0.189	1.76	1.18
D-Saccharic acid	C source	−0.00941	−0.329	−0.747	0.189
D-Gluconic acid	C source	−0.071	−0.0308	−0.562	0.344
D-Mannitol	C source	−0.379	−1.28	−1.55	0.11
D-Galacturonic acid γ-lactone	C source	−0.0335	0.223	0.213	0.475
D-Ribose	C source	−0.48	−0.4	0.609	3.15
D-Melibiose	C source	1.68	1.36	1.33	2.6
Maltotriose	C source, carbohydrate	−0.274	−0.84	−0.0948	0.0115
Acetoacetic acid	C source, carboxylic acid	−0.29	0.727	−0.151	1
Tyramine	C source, amine	−1.26	−1.15	−1.04	0.00217
D-Psicose	C source, carbohydrate	0.0227	−0.439	−0.978	0.133
D-Galacturonic acid	C source, carboxylic acid	0.301	0.241	0.601	0.896
N-Acetyl-neuramic acid	C source, carboxylic acid	−0.378	−0.478	−0.271	0.171
β-D-Allose	C source, carbohydrate	0.548	−0.153	0.744	0.97
L-Arabitol	C source, carbohydrate	−0.0865	−0.382	0.0834	0.125
Arbutin	C source, carbohydrate	−0.4	−0.239	−0.376	0.12
D-Lactitol	C source, carbohydrate	−0.0371	−0.253	−0.401	0.211
D-Glucosamine	C source, carbohydrate	−0.0519	0.471	0.878	1.42
Malonic acid	C source, carboxylic acid	0.0962	−0.423	−0.229	0.174
Quinic acid	C source, carboxylic acid	0.104	−0.282	−0.0444	0.233
N-Acetyl-L-glutamic acid	C source, amino acid	−0.0569	−0.355	−0.388	0.0138
Hydroxy-L-proline	C source, amino acid	−0.378	0.0307	0.165	0.24
DL-Octopamine	C source, amino acid	−0.375	−0.248	−1.41	0.0384
Glycine	N source, amino acid	−0.118	1.16	0.28	1.62
L-Lysine	N source, amino acid	−0.0643	−0.86	0.317	1.13
L-Serine	N source, amino acid	0.498	−0.781	−0.244	0.845
L-Threonine	N source, amino acid	−0.084	−1.13	0.418	1.34
Hydroxylamine	N source, amino acid	−0.466	0.11	−0.418	1.51
N-Amylamine	N source	−0.687	0.327	−0.245	0.957
N-Butylamine	N source	−0.608	−0.355	−0.338	1.13
Ethylamine	N source	−0.549	0.0196	−0.0643	0.651
Acetamide	N source	−0.578	−0.365	−0.446	0.881
Formamide	N source	−0.427	0.0363	−0.722	0.752
DL-Lactamide	N source	0.221	−0.0839	−0.226	0.711
D-Glucosamine	N source	0.14	1.06	0.716	1.53
D-Mannosamine	N source	0.441	0.856	0.798	1.97
Guanine	N source	−0.217	1.54	1.57	2.12
Thymine	N source	−0.641	0.287	0.0135	1.04
Thymidine	N source	−0.225	0.498	0.464	1.17
Uracil	N source	−0.415	0.288	0.257	0.47
Allantoin	N source	0.344	0.576	−0.612	0.93
Parabanic acid	N source	−0.23	0.525	0.16	1.08
Carbamyl phosphate	P source, organic	1.99	2.56	3.26	4.24
Thiophosphate	P source, inorganic	0.077	0.634	−0.594	0.867
S-Methyl-L-cysteine	S source, organic	0.209	0.57	−0.758	1.64
Cystathionine	S source, organic	0.0973	1.88	−0.565	2.2
Lanthionine	S source, organic	−0.0395	1.59	−0.643	1.8
DL-Ethionine	S source, organic	−0.0742	0.0417	−1	2.4
L-Methionine	S source, organic	0.0604	0.978	−0.659	1.83
Gly-Met	S source, organic	0.154	0.628	−0.684	3.03
N-Acetyl-DL-Methionine	S source, organic	−0.109	0.741	−0.659	2.11
DL-Lipoamide	S source, organic	−0.319	−0.168	−0.854	1.13

[a] Values were calculated as the standard deviation from the plate growth mean ($OD_{590} - OD_{750}$) as described in Materials and Methods.

The *P. fluorescens* pMP-R124 plasmid. During the assembly of the *P. fluorescens* R124 genome, we identified a scaffold sequence that did not produce any alignments of significant length to the reference genomes. In order to determine if this scaffold was a potential plasmid, we developed PCR primers that amplified outward from the 5′ and 3′ ends of the sequence. Upon amplification, these primers produced a PCR product, indicating that this molecule was a circular plasmid, which we designated pMP-R124. The plasmid sequence is 43 kbp in length, comprising 51 genes. Figure 5 highlights the regions of pMP-R124 with sequence similarity to other *Pseudomonas* plasmids and genomes. This figure highlights what appears to be two distinct regions of different

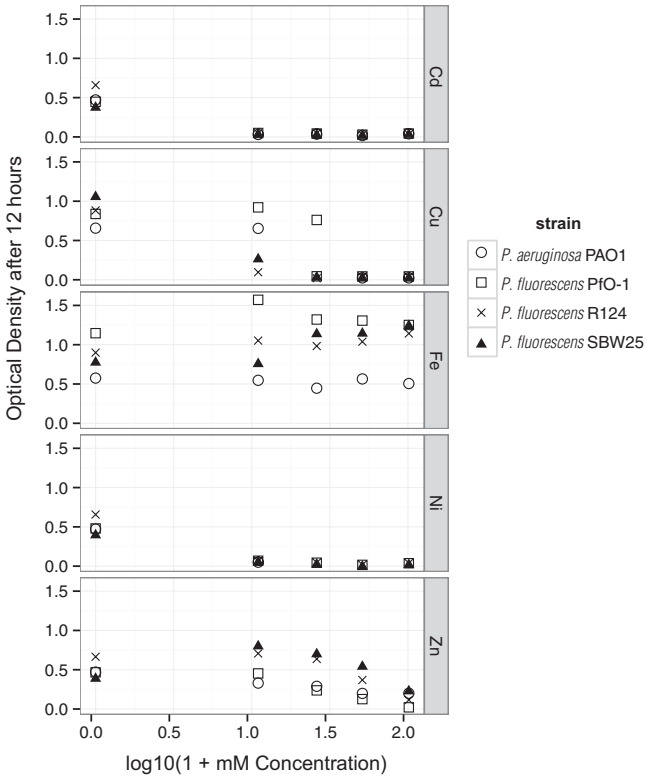

FIG 4 Growth rates of four *Pseudomonas* species in the presence of five different metals (cadmium, copper, iron, nickel, and zinc). Each datum shows a different metal concentration at which a *Pseudomonas* strain was tested.

origins within the plasmid: the largest region shares sequence similarity with several *P. syringae* plasmids (Fig. 5, blue tracks), while the second region shows similarity (mean = 40.5%) with the *P. aeruginosa* PA07 and *P. protegens* genomes (magenta track). The region within pMP-R124 demonstrating similarity to a *P. syringae* plasmid encodes a bacteriocin immunity protein and a *virB* type IV secretion operon (T4S) used by Gram-negative bacteria during conjugation (51). Sequence analysis of these genes using BLAST showed that these T4S proteins share ~55% amino acid identity with the *P. syringae* pv. maculicola plasmid ES4326A (39) and ~59% with the *P. syringae* pv. phaseolicola small plasmid 1448A (38) (see Table S8 in the supplemental material). The second smaller region within the plasmid shows limited sequence identity to regions in the *P. aeruginosa* PA07 (52) and *P. protegens* genomes. This region contains the genes *pilL* to *pilV* from the type 4b pilin system (T4Pb) (53). This system is similar to the previously described of R64 plasmid system involved in liquid and surface mating (54, 55) and the pilin genes found in the PAPI-1 self-transmission genome island in many *Pseudomonas* genomes (56, 57). These genes show, on average, more than 55% divergence from the corresponding orthologs in *P. aeruginosa* PA07 and *P. protegens* Pf-5 genomes (see Table S8 in the supplemental material).

Determining twitching motility genotype. Given the presence of the T4P genes, we decided to test *P. fluorescens* R124 for a twitching motility phenotype. We used a twitching motility (TM) assay (34) to test *P. fluorescens* R124, Pf0-1, and SBW25 against *P. aeruginosa* PAO1 as a positive control (53, 58). In our initial assays using the standard BHI medium for *Pseudomonas* twitching motility, we did not observe any phenotype for *P. fluorescens* R124. We therefore considered the possibility that environmental stressors may induce this phenotype and examined both nutritional and environmental stress. Growth on 50% LB (high salt) did not induce twitching, so we reduced the amount of carbon and energy in the plate (a 1% medium of BHI or LB). These reductions did not induce twitching motility; however, when we attempted to starve the cells of iron using King's B medium (36), a twitching phenotype was observed, but it was lost when 100 mM Fe(III) was added to the medium (data not shown), confirming the role of iron in this phenotype. The results of this analysis are shown in Fig. 6. Neither *P. fluorescens* Pf0-1 nor SBW25 demonstrated a TM phenotype under the conditions tested, while *P. aeruginosa* PAO1 demonstrated TM under all conditions, consistent with its known phenotype (58).

Given that the twitching *P. fluorescens* R124 genome shared the same T4P orthologs with the nontwitching *P. fluorescens* Pf0-1 and SBW25 strains, we considered the possibility that a TM phenotype may be related to the T4P system identified on the pMP-R124 plasmid. In order to determine if this is the case, we knocked out the pMP-R124 plasmid to create the strain R124ΔpMP-R124. This plasmidless strain demonstrated the same degree of twitching motility as the wild-type strain (Fig. 6), suggesting that it is the T4Pa genes on the genome that confer the twitching motility phenotype. We examined the clusters of homologous genes unique to the twitching motility strains to identify possible genomic loci encoding this twitching motility phenotype. However, there were no clear candidates for the observed difference in TM phenotype, and we anticipate that a more detailed phenotypic study and comparison of genomes may be required to identify them.

DISCUSSION

This study provides the genome and associated plasmid sequence of a *Pseudomonas* isolate from a mineral environment, and only the second for any microorganism isolated from a cave (15). By comparing the cave-isolated *P. fluorescens* R124 genome with that of previously sequenced *P. fluorescens* subgroup isolates, we aimed to test whether the geologic environment or nutrient limitation of the cave resulted in any phenotypic imprint on the organism. For comparison, we used *P. fluorescens* Pf0-1 and SBW25 and *P. protegens* Pf-5, which were all isolated from nutrient-rich soil environments. Two further *P. fluorescens* strains have since been sequenced (*P. fluorescens* F113 [59] and A506 [60]) but were not included in our original comparative analysis.

The *P. fluorescens* R124 genome was sequenced using a Roche/454 sequencer and assembled with <1% gaps in the final sequence. We expect these gaps to remain difficult to resolve due to repeats similar to those identified in previously sequenced *P. fluorescens* genomes (7, 9). As a result of our efforts to close gaps both manually through PCR amplification and Sanger sequencing and by *in silico* methods, we believe that this genome does represent an improved draft sequence being >99% complete across 78 scaffolded contigs.

Our initial hypothesis was that nutrient limitation within the cave environment would result in adaptation to reduce the size of the *P. fluorescens* R124 genome, as reduced genome size and essential element (P/N) costs would decrease the cost of DNA replication; however, the genome size and average gene count were similar to those of other *Pseudomonas* genomes, suggesting that

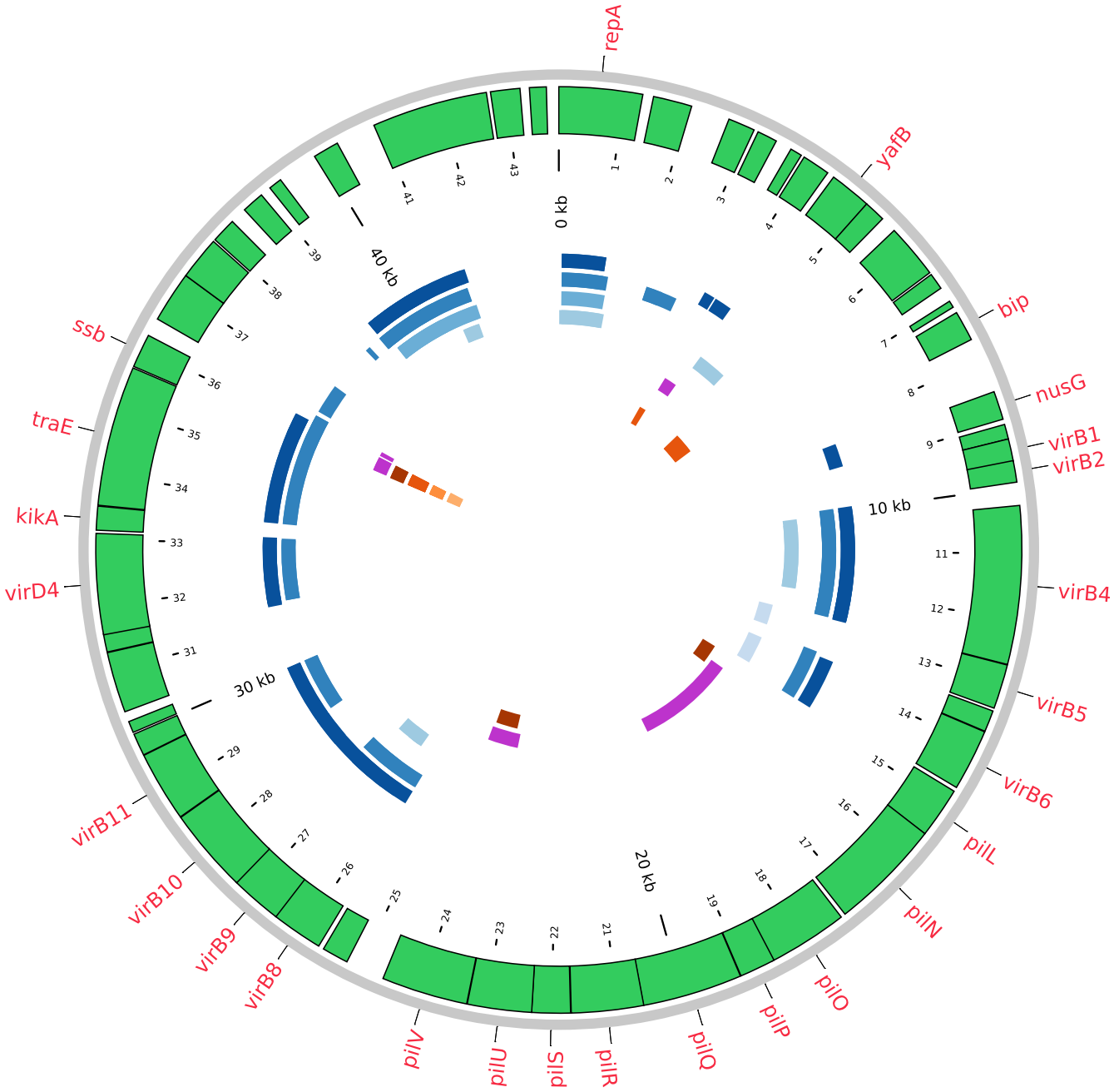

FIG 5 Map of *P. fluorescens* pMP-R124 plasmid. Genes are shown in the green outer track and labeled using sequence similarity to database sequences where possible. Inner tracks show regions of similarity to reference sequences and are color coded by type: the blue tracks represent plasmid sequences from *Pseudomonas syringae*, the purple track shows alignment to the *P. aeruginosa* PA07 genome (52), and the orange tracks represent alignments to *P. fluorescens* genomes. Amino acid identity to reference genes can be found in Table S9 in the supplemental material. The accession numbers used to generate the alignment tracks are, from outer to inner, as follows: AY603979.1, CP000060.1, AY603980.1, CP000059.1, AY603982.1, CP000744.1, CP000076.1, CP000094.2, AM181176.4, and AY887963.3.

the encountered conditions have not affected genome size or gene density.

We next questioned whether the geochemical conditions of the cave (high in reduced metals such as iron, copper, and zinc) would alter the metal-scavenging and/or protective mechanisms within *P. fluorescens* R124 (61). We compared the genes related to metal homeostasis against the reference genomes to examine whether these metal homeostasis genes in *P. fluorescens* R124 may have evolved or diverged under selective pressure for metal toxicity given the abundance of iron [0.12% (wt/wt) Fe(III)] or other heavy metals in the environment. Our analysis showed little sequence divergence across a number of metal-homeostasis systems, including iron, copper, nickel, cobalt, and cadmium, suggesting that these systems are functionality adaptive across a diverse set of environmental metal ion conditions. These genomic data were supported by the similarity in metal toxicity levels for

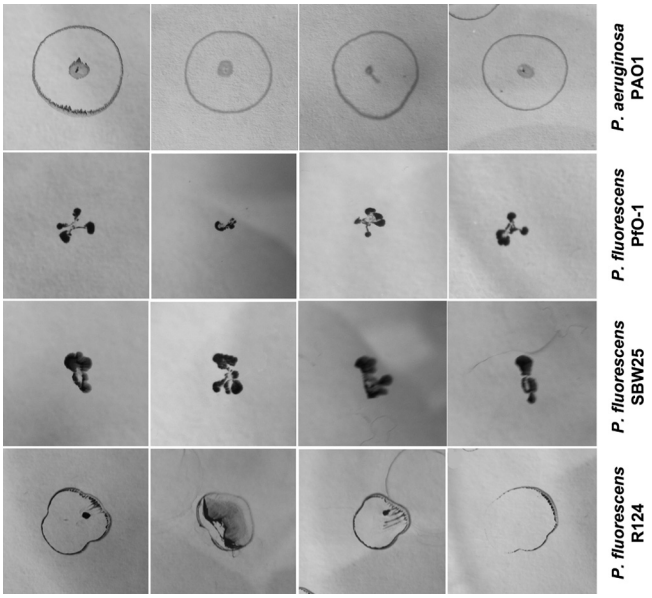

FIG 6 Twitching motility assay of the *P. fluorescens* strains Pf0-1, SBW25, and R124 and *P. aeruginosa* PAO1 (control). Each strain was incubated for 120 h at 37°C on iron-limited King's B medium (36). Each image represents an independent trial of the twitching motility assay. Crystal violet was used to stain the cells, and a positive phenotype is indicated by a circular zone of movement.

each of these strains (Fig. 4). One observable difference is the low sequence similarity in a cluster of NRPS genes in *P. fluorescens* R124 associated with siderophore export. This suggests that the core siderophore synthesis and regulation pathways are conserved but that either the siderophore structure itself has diverged or the siderophore export machinery may have been adapted for the export of a novel lipopeptide, possibly an antibiotic (41, 42); while this is an interesting finding, it is outside the scope of this study to determine what these structural changes may be and how they may have affected iron-scavenging mechanisms or lipopeptide transport.

In addition to examining the genome for mutation and adaptation, we identified several possible genomic islands acquired by horizontal gene transfer unique to *P. fluorescens* R124. Given the metabolic flexibility of pseudomonads to degrade complex organic molecules in the environment, the acquisition of these genes suggests that HGT may have expanded the cellular catabolic pathways to take advantage of presumably microbial detritus within the system, allowing this organism to play a potentially important role in carbon turnover. Indeed, in a number of cave systems, geologic isolation has led to the evolution of microbial ecosystems more dependent on chemolithotrophic energy generation and bacterially derived carbon turnover than similar microbial systems in soils (62). Nonetheless, many of the genes in these genomic islands had no annotated homologs in sequence databases, suggesting that the full range of adaptations by *P. fluorescens* R124 remains to be elucidated, an unsurprising finding given that the sequencing of greater numbers of genomes reveals increasingly greater numbers of gene families (63).

While the roles of many of the HGT genes found within the genome have yet to be resolved, *P. fluorescens* R124 contained a 43-kbp plasmid that appeared to be formed from a recombination event of two separate sequences originating from *P. aeruginosa* and *P. syringae*. The largest fragment appears to encodes replication and transfer, while the second, smaller region contained a cluster of type 4b pilin (T4Pb) genes, related to R64 liquid mating specificity (54, 64). Initially we hypothesized that these pilin genes may be responsible for the twitching motility phenotype observed in *P. fluorescens* R124; however, plasmid curing did not result in the loss of this phenotype, suggesting that TM is encoded by the genome.

By comparing the TM phenotype across three *P. fluorescens* strains, our analysis showed that only *P. fluorescens* R124 demonstrated a TM phenotype in iron-limited medium. The requirement of iron limitation was confirmed by the fact that no twitching motility phenotype was observed in *P. fluorescens* R124 when it was retested on the same medium with iron added. The *P. fluorescens* R124 TM phenotype on iron is in contrast to previous results showing that *P. fluorescens* SBW25 produces an increasing TM phenotype with the addition of $FeCl_3$ (65).

The advantage a TM phenotype conveys in the cave environment may be related to its geologic nature: previous *P. fluorescens* strains have been identified from the soil and rhizosphere, where flagellum-mediated motility would allow these organisms to explore a three-dimensional environment in search of nutrients. In contrast, within a cave, *P. fluorescens* R124 is limited to a two-dimensional rock surface. As such, TM may be a more efficient means of exploring a flatland, similar to the use of TM by other pseudomonads to explore flat leaf (48) surfaces. The specificity of iron to the *P. fluorescens* R124 TM phenotype further suggests that the activity of this phenotype is driven in response to nutrient limitation.

Together these analyses demonstrate that many gene systems within *P. fluorescens* are conserved across radically different chemical environments, suggesting flexibility of pseudomonad homeostasis and nutrient pathways to accommodate a wide range of environmental conditions. This, along with an apparent knack for acquiring environmental genes that allow adaptation to changing physical conditions, may explain why the pseudomonads have been successful in many environments.

ACKNOWLEDGMENTS

We acknowledge the students and instructors in the BIO349 class at Northern Kentucky University for their assistance in annotating *P. fluorescens* R124. We thank Mark W. Silby for providing *P. fluorescens* SBW25 and *P. fluorescens* Pf0-1 cultures, Michael L. Vasil for providing *P. aeruginosa* PAO1, Lori Burrows for her assistance with the twitching motility assay, and Barry Bocher for assistance with the Biolog assay.

This project was supported by a grant from the National Science Foundation Microbial Interactions and Processes MIP grant (0643462). DNA sequencing costs were supported by the National Center for Research Resources (5P20RR016481).

REFERENCES

1. **Hallam SJ, Putnam N, Preston CM, Detter JC, Rokhsar D, Richardson PM, DeLong EF.** 2004. Reverse methanogenesis: testing the hypothesis with environmental genomics. Science **305:**1457–1462.
2. **Marcy Y, Ouverney C, Bik EM, Losekann T, Ivanova N, Martin HG, Szeto E, Platt D, Hugenholtz P, Relman DA, Quake SR.** 2007. Dissecting biological "dark matter" with single-cell genetic analysis of rare and uncultivated TM7 microbes from the human mouth. Proc. Natl. Acad. Sci. U. S. A. **104:**11889–11894.
3. **Stepanauskas R, Sieracki ME.** 2007. Matching phylogeny and metabolism in the uncultured marine bacteria, one cell at a time. Proc. Natl. Acad. Sci. U. S. A. **104:**9052–9057.

4. **Croal LR, Gralnick JA, Malasarn D, Newman DK.** 2004. The genetics of geochemistry. Annu. Rev. Genet. **38:**175–202.
5. **Banks ED, Taylor NM, Gulley J, Lubbers BR, Giarrizzo JG, Bullen HA, Hoehler TM, Barton HA.** 2010. Bacterial calcium carbonate precipitation in cave environments: a function of calcium homeostasis. Geomicrobiol. J. **27:**444–454.
6. **Petsch ST, Eglington TI, Edwards KJ.** 2001. 14C-dead living biomass: evidence for microbial assimilation of ancient organic carbon during shale weathering. Science **292:**1127–1131.
7. **Paulsen IT, Press CM, Ravel J, Kobayashi DY, Myers GS, Mavrodi DV, DeBoy RT, Seshadri R, Ren Q, Madupu R, Dodson RJ, Durkin SS, Brinkac LM, Daugherty SC, Sullivan SA, Rosovitz MJ, Gwinn ML, Zhou L, Schneider DJ, Cartinhour SW, Nelson WC, Weidman J, Watkins K, Tran K, Khouri H, Pierson EA, Pierson LS, Thomashow LS, Loper JE.** 2005. Complete genome sequence of the plant commensal *Pseudomonas fluorescens* Pf-5. Nat. Biotechnol. **23:**873–878.
8. **Ramette A, Frapolli M, Fischer-Le Saux M, Gruffaz C, Meyer JM, Defago G, Sutra L, Moenne Loccoz Y.** 2011. *Pseudomonas protegens* sp. nov., widespread plant-protecting bacteria producing the biocontrol compounds 2,4-diacetylphloroglucinol and pyoluteorin. Syst. Appl. Microbiol. **34:**180–188.
9. **Silby MW, Cerdeno Tarraga AM, Vernikos GS, Giddens SR, Jackson RW, Preston GM, Zhang XX, Moon CD, Gehrig SM, Godfrey SA, Knight CG, Malone JG, Robinson Z, Spiers AJ, Harris S, Challis GL, Yaxley AM, Harris D, Seeger K, Murphy L, Rutter S, Squares R, Quail MA, Saunders E, Mavromatis K, Brettin TS, Bentley SD, Hothersall J, Stephens E, Thomas CM, Parkhill J, Levy SB, Rainey PB, Thomson NR.** 2009. Genomic and genetic analyses of diversity and plant interactions of *Pseudomonas fluorescens*. Genome Biol. **10:**R51. doi:10.1186/gb-2009-10-5-r51.
10. **Stover CK, Pham XQ, Erwin AL, Mizoguchi SD, Warrener P, Hickey MJ, Brinkman FS, Hufnagle WO, Kowalik DJ, Lagrou M, Garber RL, Goltry L, Tolentino E, Westbrock-Wadman S, Yuan Y, Brody LL, Coulter SN, Folger KR, Kas A, Larbig K, Lim R, Smith K, Spencer D, Wong GK, Wu Z, Paulsen IT, Reizer J, Saier MH, Hancock RE, Lory S, Olson MV.** 2000. Complete genome sequence of *Pseudomonas aeruginosa* PAO1, an opportunistic pathogen. Nature **406:**959–964.
11. **Thompson IP, Lilley AK, Ellis RJ, Bramwell PA, Bailey MJ.** 1995. Survival, colonization and dispersal of genetically modified *Pseudomonas fluorescens* SBW25 in the phytosphere of field grown sugar beet. Nat. Biotechnol. **13:**1493–1497.
12. **Howell CR, Stpianovic RD.** 1979. Control of Rhizoctonia solani on cotton seedlings with *Pseudomonas fluorescens* and with an antibiotic produced by the bacterium. Phytopathology **69:**480–482.
13. **Compeau G, Al-Achi BJ, Platsouka E, Levy SB.** 1988. Survival of rifampin-resistant mutants of *Pseudomonas fluorescens* and *Pseudomonas putida* in soil systems. Appl. Environ. Microbiol. **54:**2432–2438.
14. **Holloway BW.** 1955. Genetic recombination in *Pseudomonas aeruginosa*. J. Gen. Microbiol. **13:**572–581.
15. **Land M, Pukall R, Abt B, Goker M, Rohde M, Del Rio TG, Tice H, Copeland A, Cheng JF, Lucas S, Chen F, Nolan M, Bruce D, Goodwin L, Pitluck S, Ivanova N, Mavromatis K, Ovchinnikova G, Pati A, Chen A, Palaniappan K, Hauser L, Chang YJJ, Jefferies CC, Saunders E, Brettin T, Detter JC, Han C, Chain P, Bristow J, Eisen JA, Markowitz V, Hugenholtz P, Kyrpides NC, Klenk HP, Lapidus A.** 2009. Complete genome sequence of Beutenbergia cavernae type strain (HKI 0122). Standards Genomic Sci. **1:**21–28.
16. **Sylvia DM, Fuhrmann JJ, Hartel PG, Zuberer DA.** 2004. Principles and applications of soil microbiology, 2nd ed. Prentice Hall, Englewood Cliffs, NJ.
17. **Baker GC, Smith JJ, Cowan DA.** 2003. Review and re-analysis of domain-specific 16S primers. J. Microbiol. Methods **55:**541–555.
18. **Miller JR, Koren S, Sutton G.** 2010. Assembly algorithms for next-generation sequencing data. Genomics **95:**315–327.
19. **Markowitz VM, Mavromatis K, Ivanova NN, Chen IMM, Chu K, Kyrpides NC.** 2009. IMG ER: a system for microbial genome annotation expert review and curation. Bioinformatics **25:**2271–2278.
20. **Kurtz S, Phillippy A, Delcher AL, Smoot M, Shumway M, Antonescu C, Salzberg SL.** 2004. Versatile and open software for comparing large genomes. Genome Biol. **5:**R12. doi:10.1186/gb-2004-5-2-r12.
21. **Barton MD, Barton HA.** 2012. Scaffolder—software for manual genome scaffolding. Source Code Biol. Med. **7:**4.
22. **Barton MD, Barton HA.** 2013. Genomer—a Swiss army knife for genome scaffolding. PLoS One **8:**e66922. doi:10.1371/journal.pone.0066922.
23. **Mulet M, Lalucat J, Garcia-Valdes E.** 2010. DNA sequence-based analysis of the *Pseudomonas* species. Environ. Microbiol. **12:**1513–1530.
24. **Katoh K, Asimenos G, Toh H.** 2009. Multiple alignment of DNA sequences with MAFFT. Methods Mol. Biol. **537:**39–64.
25. **Katoh K, Toh H.** 2010. Parallelization of the MAFFT multiple sequence alignment program. Bioinformatics **26:**1899–1900.
26. **Talavera G, Castresana J.** 2007. Improvement of phylogenies after removing divergent and ambiguously aligned blocks from protein sequence alignments. Syst. Biol. **56:**564–577.
27. **Lartillot N, Lepage T, Blanquart S.** 2009. PhyloBayes 3: a Bayesian software package for phylogenetic reconstruction and molecular dating. Bioinformatics **25:**2286–2288.
28. **Rodriguez, F, Oliver JL, Marin A, Medina JR.** 1990. The general stochastic model of nucleotide substitution. J. Theor. Biol. **142:**485–501.
29. **Chin SC, Abdullah N, Siang TW, Wan HY.** 2005. Plasmid profiling and curing of Lactobacillus strains isolated from the gastrointestinal tract of chicken. J. Microbiol. **43:**251–256.
30. **Reva ON, Tummler, B.** 2004. Global features of sequences of bacterial chromosomes, plasmids and phages revealed by analysis of oligonucleotide usage patterns. BMC Bioinformatics **5:**90.
31. **Reva ON, Tummler, B.** 2005. Differentiation of regions with atypical oligonucleotide composition in bacterial genomes. BMC Bioinformatics **6:**251.
32. **R Development Core Team.** 2005. R: a language and environment for statistical computing. R Foundation for Statistical Computing, Vienna, Austria.
33. **Bochner BR, Gadzinski P, Panomitros E.** 2001. Phenotype microarrays for high-throughput phenotypic testing and assay of gene function. Genome Res. **11:**1246–1255.
34. **Gallant CV, Daniels C, Leung JM, Ghosh AS, Young KD, Kotra LP, Burrows LL.** 2005. Common beta-lactamases inhibit bacterial biofilm formation. Mol. Microbiol. **58:**1012–1024.
35. **Koo J, Tammam S, Ku SY, Sampaleanu LM, Burrows LL, Howell PL.** 2008. PilF is an outer membrane lipoprotein required for multimerization and localization of the *Pseudomonas aeruginosa* type IV pilus secretin. J. Bacteriol. **190:**6961–6969.
36. **King EO, Ward MK, Raney DE.** 1954. Two simple media for the demonstration of pyocyanin and fluorescin. J. Lab. Clin. Med. **44:**301–307.
37. **Field D, Garrity G, Gray T, Morrison N, Selengut J, Sterk P, Tatusova T, Thomson N, Allen MJ, Angiuoli SV, Ashburner M, Axelrod N, Baldauf S, Ballard S, Boore J, Cochrane G, Cole J, Dawyndt P, De Vos P, DePamphilis C, Edwards R, Faruque N, Feldman R, Gilbert J, Gilna P, Oliver F, Goldstein P, Guralnick R, Haft D, Hancock D, Hermjakob H, Hertz-Fowler C, Hugenholtz P, Joint I, Kagan L, Kane M, Kennedy J, Kowalchuk G, Kottmann R, Kolker E, Kravitz S, Kyrpides N, Leebens-Mack J, Lewis SE, Li K, Lister AL, Lord P, Maltsev N, Markowitz V, Martiny J, Methe B, et al.** 2008. The minimum information about a genome sequence (MIGS) specification. Nat. Biotechnol. **26:**541–547.
38. **Joardar V, Lindeberg M, Jackson RW, Selengut J, Dodson R, Brinkac LM, Daugherty SC, Deboy R, Durkin SS, Gwinn M, Madupu R, Nelson WC, Rosovitz MJ, Sullivan S, Crabtree J, Creasy T, Davidsen T, Haft DH, Zafar N, Zhou L, Halpin R, Holley T, Khouri H, Feldblyum T, White O, Fraser CM, Chatterjee AK, Cartinhour S, Schneider DJ, Mansfield J, Collmer A, Buell RR.** 2005. Whole-genome sequence analysis of *Pseudomonas syringae* pv. phaseolicola 1448A reveals divergence among pathovars in genes involved in virulence and transposition. J. Bacteriol. **187:**6488–6498.
39. **Stavrinides J, Guttman DS.** 2004. Nucleotide sequence and evolution of the five-plasmid complement of the phytopathogen *Pseudomonas syringae* pv. maculicola ES4326. J. Bacteriol. **186:**5101–5115.
40. **Chai LC, Hong BH, Elemfareji OI, Thong KL.** 2012. Variable carbon catabolism among Salmonella enterica serovar Typhi isolates. PLoS One **7:**e36201. doi:10.1371/journal.pone.0036201.
41. **Moon CD, Zhang XX, Matthijs S, Schafer M, Budzikiewicz H, Rainey PB.** 2008. Genomic, genetic and structural analysis of pyoverdine-mediated iron acquisition in the plant growth-promoting bacterium *Pseudomonas fluorescens* SBW25. BMC Microbiol. **8:**7.
42. **Ravel J, Cornelis P.** 2003. Genomics of pyoverdine-mediated iron uptake in pseudomonads. Trends Microbiol. **11:**195–200.
43. **Hartney SL, Mazurier S, Kidarsa TA, Carolina M, Lemanceau P, Loper**

JE. 2011. TonB-dependent outer-membrane proteins and siderophore utilization in *Pseudomonas fluorescens* Pf-5. Biometals **24:**193–213.
44. **Canovas D, Cases I, de Lorenzo V.** 2003. Heavy metal tolerance and metal homeostasis in *Pseudomonas* putida as revealed by complete genome analysis. Environ. Microbiol. **5:**1242–1256.
45. **Outten FW, Huffman DL, Hale JA, O'Halloran TV.** 2001. The independent cue and cus systems confer copper tolerance during aerobic and anaerobic growth in Escherichia coli. J. Biol. Chem. **276:**30670–30677.
46. **Solioz, M., Stoyanov, J. V.** 2003. Copper homeostasis in Enterococcus hirae. FEMS Microbiol. Rev. **27:**183–195.
47. **Zhang XX, Rainey PB.** 2008. Regulation of copper homeostasis in *Pseudomonas fluorescens* SBW25. Environ. Microbiol. **10:**3284–3294.
48. **Gibiansky ML, Conrad JC, Jin F, Gordon VD, Motto DA, Mathewson MA, Stopka WG, Zelasko DC, Shrout JD, Wong GCL.** 2010. Bacteria use type IV pili to walk upright and detach from surfaces. Science **330:**197.
49. **Yan Y, Yang J, Dou Y, Chen M, Ping S, Peng J, Lu W, Zhang W, Yao Z, Li H, Liu W, He S, Geng L, Zhang X, Yang F, Yu H, Zhan Y, Li D, Lin Z, Wang Y, Elmerich C, Lin M, Jin Q.** 2008. Nitrogen fixation island and rhizosphere competence traits in the genome of root-associated *Pseudomonas stutzeri* A1501. Proc. Natl. Acad. Sci. U. S. A. **105:**7564–7569.
50. **Daum M, Zimmer W, Papen H, Kloos K, Nawrath K, Bothe H.** 1998. Physiological and molecular biological characterization of ammonia oxidation of the heterotrophic nitrifier *Pseudomonas* putida. Curr. Microbiol. **37:**281–288.
51. **Wallden K, Rivera-Calzada A, Waksman G.** 2010. Microreview: Type IV secretion systems: versatility and diversity in function. Cell. Microbiol. **12:**1203–1212.
52. **Roy PH, Tetu SG, Larouche A, Elbourne L, Tremblay S, Ren Q, Dodson R, Harkins D, Shay R, Watkins K, Mahamoud Y, Paulsen IT.** 2010. Complete genome sequence of the multiresistant taxonomic outlier *Pseudomonas aeruginosa* PA7. PLoS One **5:**e8842. doi:10.1371/journal.pone.0008842.
53. **Mattick JS.** 2002. Type IV pili and twitching motility. Annu. Rev. Microbiol. **56:**289–314.
54. **Kim SR, Komano T.** 1997. The plasmid R64 thin pilus identified as a type IV pilus. J. Bacteriol. **179:**3594–3603.
55. **Sampei GI, Furuya N, Tachibana K, Saitou Y, Suzuki T, Mizobuchi K, Komano T.** 2010. Complete genome sequence of the incompatibility group I1 plasmid R64. Plasmid **64:**92–103.
56. **Mavrodi DV, Loper JE, Paulsen IT, Thomashow LS.** 2009. Mobile genetic elements in the genome of the beneficial rhizobacterium *Pseudomonas fluorescens* Pf-5. BMC Microbiol. **9:**8.
57. **Carter MQ, Chen J, Lory S.** 2010. The *Pseudomonas aeruginosa* pathogenicity island PAPI-1 is transferred via a novel type IV pilus. J. Bacteriol. **192:**3249–3258.
58. **Ayers M.** 2009. PilM/N/O/P proteins form an inner membrane complex that affects the stability of the *Pseudomonas aeruginosa* type IV pilus secretin. J. Mol. Biol. **394:**128–142.
59. **Redondo-Nieto M, Barret M, Morrisey JP, Germaine K, Martinez-Granero F, Barahona E, Navazo A, Sanchez-Contreras M, Moynihan JA, Giddens SR, Coppoolse ER, Muriel C, Stiekema WJ, Rainey PB, Dowling D, O'Gara F, Martin M, Rivilla R.** 2012. Genome sequence of the biocontrol strain *Pseudomonas fluorescens* F113. J. Bacteriol. **194:**1273–1274.
60. **Loper JE, Hassan KA, Mavrodi DV, Davis EW, Kent C, Shaffer BT, Elbourne LD, Stockwell VO, Hartney SL, Breakwell K, Henkels MD, Tetu SG, Rangel LI, Kidarsa TA, Wilson NL, van de Mortel JE, Song C, Blumhagen R, Radune D, Hostetler JB, Brinkac LM, Durkin SS, Kluepfel DA, Wechter PP, Anderson AJ, Cheol Y, Pierson LS, Pierson EA, Lindow SE, Kobayashi DY, Raaijmakers JM, Weller DM, Thomashow LS, Allen AE, Paulsen IT.** 2012. Comparative genomics of plant-associated *Pseudomonas* spp.: insights into diversity and inheritance of traits involved in multitrophic interactions. PLoS Genet. **8:**e1002784. doi:10.1371/journal.pgen.1002784.
61. **Schalk IJ, Hannauer M, Braud A.** 2011. New roles for bacterial siderophores in metal transport and tolerance. Environ. Microbiol. **13:**2844–2854.
62. **Engel ASS, Meisinger DB, Porter ML, Payn RA, Schmid M, Stern LA, Schleifer KH, Lee NM.** 2010. Linking phylogenetic and functional diversity to nutrient spiraling in microbial mats from Lower Kane Cave (U. S. A.). ISME J. **4:**98–110.
63. **Kislyuk A, Haegeman B, Bergman N, Weitz J.** 2011. Genomic fluidity: an integrative view of gene diversity within microbial populations. BMC Genomics **12:**32.
64. **Pelicic V.** 2008. Type IV pili: e pluribus unum? Mol. Microbiol. **68:**827–837.
65. **Koza A, Hallett PD, Moon CD, Spiers AJ.** 2009. Characterization of a novel air-liquid interface biofilm of *Pseudomonas fluorescens* SBW25. Microbiology **155:**1397–1406.